JOURNAL OF PROPULSION AND POWER
Vol. 14, No. 6, November–December 1998

Three-Dimensional Flow Theory of Turbomachinery, Part 2: Design and Analysis System

Jianzhong Xu,* Manchu Ge,† Xiaolu Zhao,† and Zhengming Wang†
Chinese Academy of Sciences, 100080 Beijing, People's Republic of China

This is the second part of a two-part paper (see "Three-Dimensional Flow Theory of Turbomachinery, Part 1: Basic Methodology," *Journal of Propulsion and Power*, Vol. 14, No. 6, 1998, pp. 899–906). The quasi-three-dimensional design and analysis system of a three-dimensional flow theory and its new application in China is introduced. A brief review on the methods associated with the solutions of quasi- and fully three-dimensional flow in subsonic and transonic turbomachines, including inverse problems, is given. A comparison of the computational results based on this system with experimental data is also made in this paper.

Nomenclature

$A_1, A_2, A_3, A_4, A_5, A_6$ = coefficient in dynamic equation
a_{ij} = covariant component of two-dimensional metric tensor
$\boldsymbol{e}$ = vector
e^i = contravariant component of $\boldsymbol{e}$
F = force acting on S_2 surface per unit mass of fluid
g^{jk} = contravariant component of three-dimensional metric tensor
g_{jk} = covariant component of three-dimensional metric tensor
H = stagnation enthalpy
I = stagnation rothalpy
l = mixing length or generator of the surface of revolution
l, φ = orthogonal coordinates on surface of revolution
M = Mach number
$\boldsymbol{n}$ = unit vector normal to stream surface
n_i = covariant component of $\boldsymbol{n}$
Pr = Prandtl number
p = pressure
q = any flow quantity
R = gas constant
r, φ, z = relative cylinder coordinates
s = entropy
T = temperature
t = time
u = tangential velocity component
$\boldsymbol{V}$ = absolute velocity vector
$V_\theta r$ = angular momentum of fluid about axis of rotation
$\boldsymbol{W}$ = relative velocity vector
w^i = contravariant component of $\boldsymbol{W}$
w_i = covariant component of $\boldsymbol{W}$
x^i = arbitrary curvilinear coordinate
z = axial coordinate
ε = dissipation rate
η = coordinate used for calculation
θ = angle between x^1 and x^2 coordinates
κ = specific heat ratio or turbulent kinetic energy
λ = heat conduction coefficient
μ = dynamic viscosity
ν = coefficient of kinetic viscosity
ξ = coordinate used for calculation
π' = stress tensor
ρ = density
σ = angle between the flow and axial direction along meridional plane
τ = viscous stress
$\tilde{\tau}$ = normal distance between two adjacent stream surfaces
Φ = dissipation function or angle between flow and curvilinear coordinate
φ = tangential coordinate
ψ = stream function
ω = angular velocity

Subscripts

j = along the x^1 coordinate
k = along the x^2 coordinate
r, φ, z = radial, circumferential, and axial component
θ = absolute tangential direction
φ = relative tangential direction

Superscript

$-$ = on stream surface or dimensionless quantity

I. Introduction

In the three-dimensional flow theory of turbomachinery, a fully three-dimensional flow solution is obtained from iterative calculations between a number of S_1 and S_2 stream surfaces, whereas a quasi-three-dimensional solution is obtained by iterative calculations between a number of S_1 surfaces of revolution and a central S_2 surface. To take account of the viscosity effect, a boundary-layer calculation is either added to the computation on one kind of stream surface and then iterated with the calculations on another kind of stream surface, or directly added to the three-dimensional inviscid flow solution and iterated with the latter.

After an experience in quasi- and fully three-dimensional solutions[1] for a single-stage research axial compressor,[2] an it-

Presented as Paper 95-7000 at the 12th International Symposium on Air Breathing Engines, Melbourne, Australia, March 20–23, 1995; received Jan. 5, 1996; revision received April 20, 1998; accepted for publication May 5, 1998.

*Academician, Institute of Engineering Thermophysics, P.O. Box 2706.
†Professor, Institute of Engineering Thermophysics, P.O. Box 2706.

erative calculation on a centrifugal compressor rotor was performed.[3,4]

The principal equation of ψ takes the following form[3]:

$$\frac{\partial}{\partial x^2}\left[\frac{1}{\rho}\left(\frac{g_{11}}{\sqrt{g}}\frac{\partial\psi}{\partial x^2}-\frac{g_{12}}{\sqrt{g}}\frac{\partial\psi}{\partial x^1}\right)\right]-\frac{\partial}{\partial x^1}\left[\frac{1}{\rho}\left(\frac{g_{12}}{\sqrt{g}}\frac{\partial\psi}{\partial x^2}-\frac{g_{22}}{\sqrt{g}}\frac{\partial\psi}{\partial x^1}\right)\right]=-2\omega\frac{D(\varphi,r)}{D(x^1,x^2)}-\frac{\sqrt{g_{11}}}{w^1}\left(\frac{\partial I}{\partial x^2}-T\frac{\partial s}{\partial x^2}\right) \tag{1}$$

where the x^3 line is located on the meridional plane and is normal to the intersecting line of the S_1 surface and the meridional plane, and

$$\frac{D(\varphi,r)}{D(x^1,x^2)}=\begin{bmatrix}\dfrac{\partial r}{\partial x^1} & r\dfrac{\partial\varphi}{\partial x^1}\\ \dfrac{\partial r}{\partial x^2} & r\dfrac{\partial\varphi}{\partial x^2}\end{bmatrix}$$

For a quasi-three-dimensional solution, the iterative calculation begins with the computation on the central S_2 surface. While for a fully three-dimensional solution, consecutive iterative calculation is performed on eight S_1 surfaces and seven S_2 surfaces. After four cycles of iteration, the maximum relative error in the Mach number is reduced to 12%. The computed meridional velocity for the Krain impeller[5] is compared with the quasi-three-dimensional solution, the Navier–Stokes[6] solution, as well as the measured data (Fig. 1). The difference between the quasi- and the fully three-dimensional solutions in section IV is small, and none have predicted the existence of the separated region, though some regions of low kinetic energy is found in the Navier–Stokes solution. At the exit section of the impeller, the fully three-dimensional result is closer to the experimental data than the quasi-three-dimensional results because the twist of the S_1 surface and the circumferential variation of the thickness of S_1 stream filaments are considered in the former and neglected in the latter.

It is interesting to note the shape change of S_1 and S_2 surfaces during the iterative process. The maximum deviation of the S_1 surface from the revolutional surface in the circumferential direction appears near the pressure side and in the midspan of the blade (Fig. 2).

The maximum tangential variation of the thickness of the S_1 stream filament occurs at the casing and hub. The deviation of

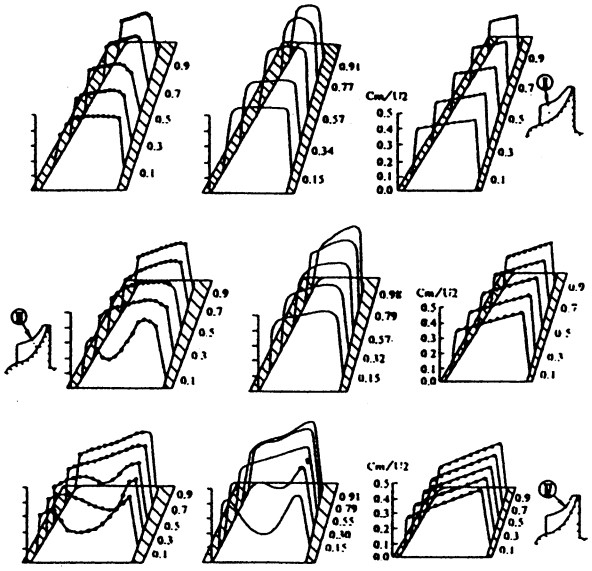

Fig. 1 Comparison of meridional velocity distributions.

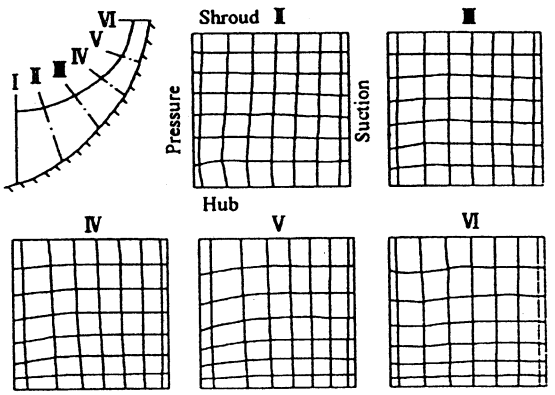

Fig. 2 Shapes of S_1 and S_2 stream surfaces of Krain impeller.

the S_1 stream surface may be predicted by the following relation[7]:

$$\frac{\partial\sigma}{r\partial\varphi}=\frac{1}{W_i}\left[\frac{\partial(V_\theta r)}{\partial n}\right]-\xi_i \tag{2}$$

where $\sigma = tg^{-1}(W_r/W_z)$, ξ is the absolute vorticity. The computational results for the twist of the S_1 surface agree well with Eq. (2). The maximum relative deviation for a centrifugal impeller is about 10%, whereas it is only about 1% for an axial compressor. In spite of the large deviation in the centrifugal compressor, the deference between the quasi- and fully three-dimensional solutions is not as large as expected. This is most likely because the inviscid secondary flow effect ignored in the quasi-three-dimensional computation is much less than the viscous effect.

II. Methods of Solving Inverse Design Problem on the Stream Surfaces

There are three types of aerothermodynamic problems: direct, inverse, and mixed. The difference in the last two types lies in that no constraint on the geometry is imposed for the geometry determination based on a specified parameter distribution in the inverse problem, whereas some constraints on geometry together with a prescribed parameter distribution are imposed in obtaining the geometry in the design problem. Both types are named as the inverse design problem in the text.

As an important part of the three-dimensional flow theory in turbomachinery, the inverse design problem has been investigated in recent years. Many methods for solving this type of problem on two kinds of stream surfaces have been developed, including the mean streamline method and the mean stream surface method discussed earlier.

These methods may be classified as decoupled-solution,[8–11] inversion method,[2–17] and variational.[18,19]

A. Decoupled-Solution Method

In this method, the flow variables and the geometric coordinates are decoupled during the solution process. The calculation starts with an initial guess for the blade geometry to be determined. A boundary-value problem is then solved for the given blade profile. A velocity distribution on the blade surface dependent of the given geometry is then obtained from the solution of this boundary-value problem.

The principal equation of the stream function on a stream surface of revolution is

$$\frac{\partial}{\partial x^1}\left[\frac{\sqrt{a_{22}}}{\tau\rho\sin\theta_{12}}\left(\frac{1}{\sqrt{a_{11}}}\frac{\partial\psi}{\partial x^1}-\frac{\cos\theta_{12}}{\sqrt{a_{22}}}\frac{\partial\psi}{\partial x^2}\right)\right]+\frac{\partial}{\partial x^2}\left[\frac{\sqrt{a_{11}}}{\tau\rho\sin\theta_{12}}\left(\frac{1}{\sqrt{a_{22}}}\frac{\partial\psi}{\partial x^2}-\frac{\cos\theta_{12}}{\sqrt{a_{11}}}\frac{\partial\psi}{\partial x^1}\right)\right]=2\sqrt{a_{11}a_{22}}\sin\sigma\sin\theta_{12} \tag{3}$$

For a fully inverse problem on a surface of revolution, in addition to the shape of the stream surface and its corresponding stream filament thickness, the inlet flow parameters and the velocity distribution on the cascade surfaces are specified. The values of the stream function on the given blade surface may be computed by the following relations which are derived from the continuity equation:

$$\psi_p = \psi_{j,1} = \psi_{j,2} - (\Delta x^2)(W_p)_j \tau_j \rho_{j,1} (\sqrt{a_{22}})_{j,1} \sin(\theta_{12})_{j,1} \quad (4)$$

$$\psi_s = \psi_{j,N} = \psi_{j,N-1} - (\Delta x^2)(W_s)_j \tau_j \rho_{j,N} (\sqrt{a_{22}})_{j,N} \sin(\theta_{12})_{j,N} \quad (5)$$

Thus, it is a boundary-value problem of von Neumann type. The new blade surfaces corresponding to $\psi = 0$ and $\psi = \Delta\psi$ can be obtained. After construction of the update grid system in this new cascade channel from the solution of the values of ψ and ρ at the new grid points may be computed. The values of ψ on the new geometry may be also computed. A new cycle of calculation begins. This process continues until the maximum relative error of the coordinates between two adjacent cycles is less than a prescribed value.

For the mixed-type problem, the solution method is similar to that for the fully inverse problem. The only difference lies in the constraint of the given distribution of the circumferential blade thickness for new blade geometry.

As an example, the velocity distribution of the T_1 cascade[20] computed from the direct problem is used as the input data for the inverse problem. The blade profile obtained from the solution for the inverse problem is in good accordance with the original geometry (Fig. 3).

Taking account of the gas viscosity effect, a method of solving the inverse design problem with the aid of an inviscid–viscous flow iteration is developed.[10] In the calculation, following the solutions of the inviscid inverse problem, the corresponding boundary problem can be solved to obtain coordinates of the cascade surfaces, and the given distribution of velocity on the cascade surfaces is considered to be located at the boundary formed by the original one and the displacement thickness. The problem is then converted to solving the inviscid inverse problem according to the prescribed distribution of velocity along the new boundary.

By use of this method the new coordinates of the modified T_1 cascade is obtained (Fig. 4) in accordance with the improved distribution of the Mach number along the T_1 cascade (Fig. 5). The maximum deviation of the coordinates in the inviscid inverse problem from that consisting of the original T_1 cascade and the displacement thickness in the preceding cycle is less than 0.01 mm, whereas after three cycles it becomes 0.03 mm. This shows that three cycles are enough for the usual engineering design.

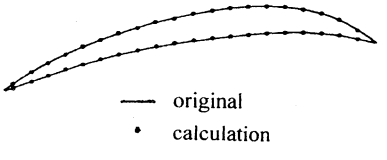

Fig. 3 Comparison of calculated and original cascade coordinates.

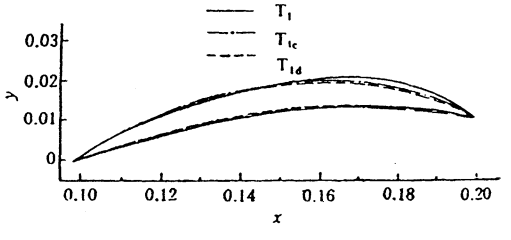

Fig. 4 Original and modified cascade coordinates.

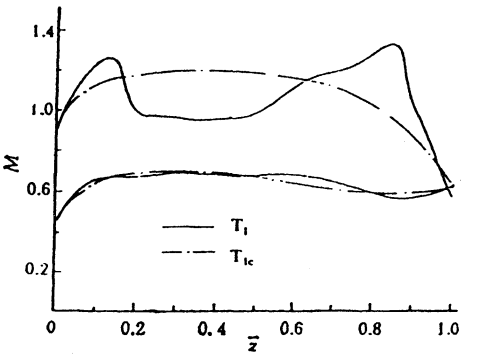

Fig. 5 Original and modified Mach number distributions on T_1 cascade surfaces.

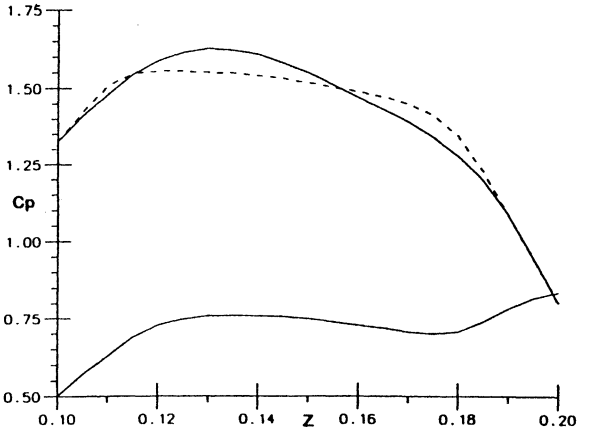

Fig. 6 Target pressure coefficient distributions.

A method to solve the inverse problem with the aid of Navier–Stokes equations was proposed.[11] The governing equations in the divergence form expressed with respect to nonorthogonal coordinates and its corresponding nonorthogonal velocity components are used[21]:

$$\frac{\partial(\sqrt{g}\rho)}{\partial t} + \frac{\partial}{\partial x^i}\left(\sqrt{\frac{g}{g_{ii}}}\,\rho w^i\right) = 0 \quad (6)$$

$$\frac{\partial}{\partial t}\left(\sqrt{\frac{g}{g_{ii}}}\,\rho w^j \boldsymbol{e}_j\right) + \frac{\partial}{\partial x^i}\left(\sqrt{\frac{g}{g_{ii}g_{jj}}}\,w^i w^j \boldsymbol{e}_j\right) + \frac{\partial}{\partial x^i}(\sqrt{g}p\boldsymbol{e}^i) + \frac{\partial}{\partial x^i}(-\pi_{j\alpha} g^{\alpha i}\sqrt{g}\boldsymbol{e}^i) = 0 \quad (7)$$

$$\frac{\partial}{\partial t}[\sqrt{g}(\rho H - p)] + \frac{\partial}{\partial x^i}\left(\sqrt{\frac{g}{g_{ii}}}\,\rho w^i H\right) + \frac{\partial}{\partial x^i}\left(-\sqrt{g}g^{ij}\lambda\frac{\partial T}{\partial x^j}\right) + \frac{\partial}{\partial x^i}\left(-\sqrt{\frac{g}{g_{kk}}}\,g^{ij}\pi_k w^k\right) = 0 \quad (8)$$

where x^1 and x^2 are circumferential and quasistreamwise directions, respectively.

In the inverse problem, the pressure distributions along the cascade surfaces derived from the distribution of the target pressure coefficient are given, W is taken as zero and W is computed from the solution of Navier–Stokes equations. In the computation the cascade surfaces to be determined are changed continuously until convergence.

Computed coordinates of the two cascades corresponding to the target distributions of the pressure coefficient (Fig. 6) are

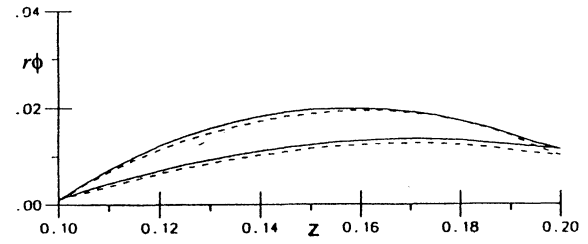

Fig. 7 Cascade coordinates calculated by the inverse problem.

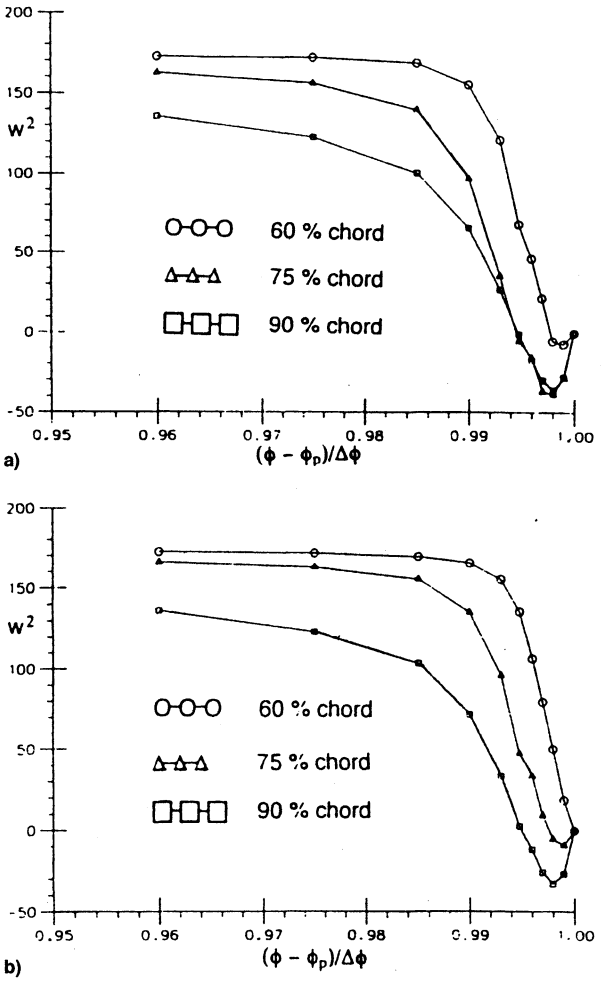

Fig. 8 Velocity profiles at different axial locations in the cascade channel.

shown in Fig. 7. In this calculation a Baldwin–Lomax turbulence model[22] is used and the MacCormack explicit scheme[23] is adopted. From the velocity distributions on the different axial locations (Fig. 8) it is seen that along the first cascade the initial separation occurs at the point of 60% chord length, while for the second one it happens at 75% chord. This indicates that the calculation of the inverse problem may give a way to delay the separation along the cascade and is very useful in aerodynamic design.

B. Method of Inversion

The method of inversion is to solve the governing equations of the inverse problem directly. In aerothermodynamics, the gas variables are usually expressed as functions of the coordinates, and the basic equations of motion are all partial differential equations with the coordinates. In the inverse problem, the coordinates are unknown and one of them is taken as a function of another coordinate and one gas parameter. The basic equations of motion are inversed to a partial differential equation in which another coordinate and the gas parameter are the independent variables. Taking the stream function method as an example, the stream function $\psi(x^1, x^2)$ and its principal equation $L\,\psi(x^1, x^2) = 0$ are inverted to one coordinate $x^2\,(x^1, \psi)$ and the coordinate-system function equation $Lx^2\,(x^1, \psi) = 0$, separately.

For the inverse problem on the surface of revolution, the corresponding coordinate stream function equation now takes the form

$$A_1\frac{\partial^2(r\varphi)}{\partial x^1\partial x^1} + A_2\frac{\partial^2(r\varphi)}{\partial x^1\partial x^2} + A_3\frac{\partial^2(r\varphi)}{\partial x^2\partial x^2} + A_4\frac{\partial(r\varphi)}{\partial x^1} + A_5\frac{\partial(r\varphi)}{\partial x^2} = A_6 \tag{9}$$

where

$$A_1 = \sqrt{g_{22}}, \qquad A_2 = \mp 2\sqrt{g_{11} - 1} - \frac{n_1 n_2}{n_3 n_3}\frac{1}{\sqrt{g_{22}}}$$

$$A_3 = \left[g_{11} + \left(\frac{n_1}{n_3}\right)^2\right]\Big/\sqrt{g_{22}}$$

$$A_4 = \pm\sqrt{g_{11} - 1}\left[\frac{\overline{\partial(\ell n\ \tau\rho)}}{\partial x^2} - \frac{\overline{\partial^2\psi}}{\partial x^2\partial x^2}\Big/\frac{\overline{\partial\psi}}{\partial x^2}\right]$$

$$A_5 = \mp\sqrt{g_{11} - 1}\,\frac{\overline{\partial(\ell n\ \tau\rho)}}{\partial x^2}$$

$$A_6 = \left\{-\tau\left[2\omega\left(\frac{n_1}{n_3}\cos\Phi_1\sqrt{g_{22}} + \frac{n_2}{n_3}\cos\Phi_2\sqrt{g_{11}}\right) + \frac{1}{W^1}\left(\frac{\overline{\partial I}}{\partial x^2} - T\frac{\overline{\partial s}}{\partial x^2}\right)\right] + \left[1 + \left(\frac{n_1}{n_3}\right)^2\right]\cdot\frac{\overline{\partial^2\psi}}{\partial x^2\partial x^2}\right\}$$

$$\Big/\frac{\overline{\partial\psi}}{\partial x^2} - \frac{\partial}{\partial x^1}\left\{\frac{n_1 n_2}{n_3 n_3} + 2\frac{n_1}{n_3}\frac{\overline{\partial(n_1/n_3)}}{\partial x^2} + \frac{n_1 n_2}{n_3 n_3}\frac{\overline{\partial(\ell n\ \tau\rho)}}{\partial x^1} - \left[1 + \left(\frac{n_1}{n_3}\right)^2\frac{\overline{\partial(\ell n\ \tau\rho)}}{\partial x^2}\right]\right\}$$

The first roots in these expressions are chosen for $\theta_{12} \le 90$ deg, and the second ones for $\theta_{12} > 90$ deg.

This is also a boundary-value problem of von Neumann type and may be solved for both full inverse and mixed-type problems. The coordinates of the cascades in accordance with the distributions of Mach number in Fig. 9 are computed from the

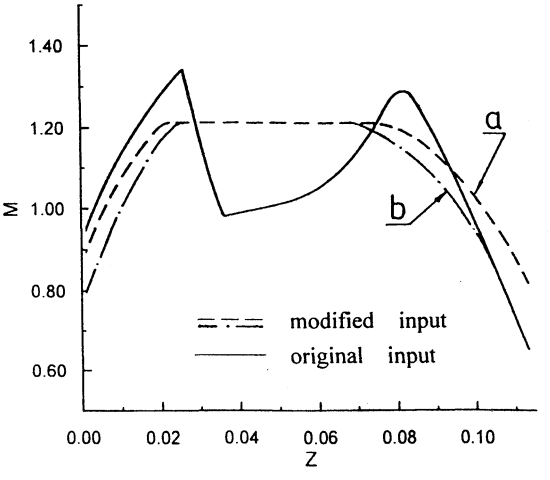

Fig. 9 Original and modified Mach number distributions on T_1 cascade surfaces.

discretized equation of Eq. (9) and shown in Fig. 10. The advanatage of this method is the simplicity and effectiveness of its computation.

When the inviscid–viscous iteration is combined with the method of inversion, the cascade coordinates obtained in the inviscid calculation are taken as the boundaries and the boundary-layer equations are solved in this region. After the mass flux in the boundary layer is computed out, it is used as the new mass flux to start the next cycle of calculation until a convergent solution is obtained. In this procedure, to guarantee the work done by the cascade, it is necessary to adjust the exist flow angle making the Kutta condition satisfied.

For the S_2 surface, the formulation of the inverse problem is to solve the geometric coordinates of the inner and outer walls of the stream surface with the given distributions of certain flow variables and the $V_\theta r$ values in the whole flow domain. In the mixed-type problem, the geometric parameters on one wall together with the $V_\theta r$ field and the distribution of one flow variable along the wall to be determined are specified. The principal equation for the inverse design problem on the S_2 surface may be derived by the method of inversion:

$$A_1 \frac{\partial^2 r}{\partial x^1 \partial x^1} + A_2 \frac{\partial^2 r}{\partial x^1 \partial x^2} + A_3 \frac{\partial^2 r}{\partial x^2 \partial x^2} + A_4 \frac{\partial r}{\partial x^1} + A_5 \frac{\partial r}{\partial x^2} = A_6 \tag{10}$$

where $A_1, \ldots, A_5$ are the functions of the geometric parameters and their first-order derivatives with r

$$A_6 = -D1 \left(\frac{\partial z}{\partial x^1}\right)^2 + D2 \frac{\partial z}{\partial x^1}\frac{\partial z}{\partial x^2} - \frac{\partial z}{\partial x^2}\frac{\partial^2 z}{\partial x^2 \partial x^2} + \left[\frac{n_2}{n_3}\frac{\partial (V_\theta r)}{\partial x^1} - \frac{n_1}{n_3}\frac{\partial (V_\theta r)}{\partial x^2}\right] \tau' \sqrt{g_{11} g_{22}}$$

and $D1$ and $D2$ are the functions of the geometric parameters and their first-order derivatives of z. The corresponding discretized equation may be solved by the line relaxation method.

The flow path of a single axial compressor is computed with the aid of the present method (Figs. 11 and 12). It is seen that the change in the distribution of velocity along the walls has a strong influence on the shape of the flow path, which can greatly influence the performance of turbomachinery.

C. Controlled Diffusion Cascade

The previously mentioned methods of solving the inverse design problem may be widely used in the three-dimensional design of turbomachinery as well as in the aerodynamic design of cascade. For the latter case, the controlled diffusion cascade may be designed and investigated by the method for the inverse design problem.

Actually, this method with a given desirable pressure distribution along the cascade surfaces is an efficient design tool for the controlled diffusion cascade, and the desirable pressure distribution may yield supercritical flow in many cases.

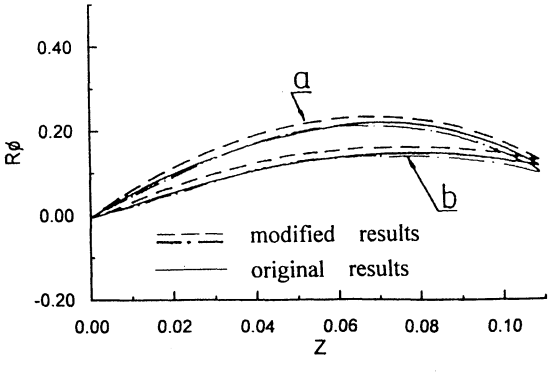

Fig. 10 Original and modified cascade coordinates.

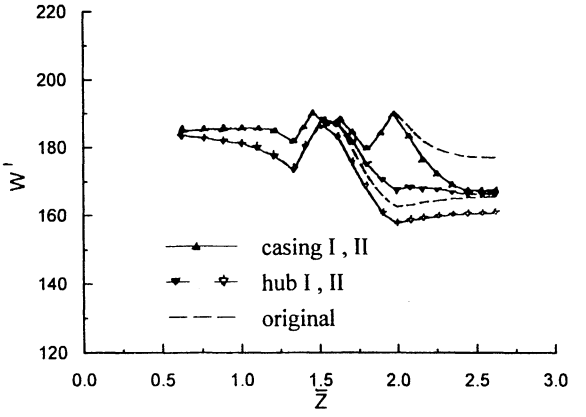

Fig. 11 Velocity profiles at the walls.

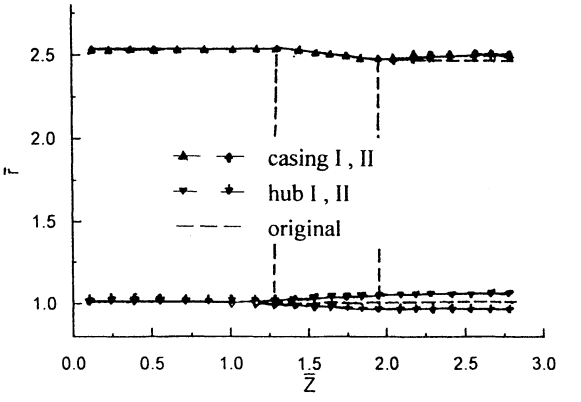

Fig. 12 Calculated coordinates of the flow path.

In the computation procedure it is assumed that the velocity distribution along the outer edge of the boundary layer is identical with that in an inviscid flow on the surface consisting of the cascade surface and the displacement thickness, and the pressure distribution along the cascade surface may be converted to the velocity distribution at the outer edge of the boundary layer with the assumption of the constant pressure in the normal direction to the cascade surface:

$$W = \sqrt{\frac{2k}{k-1}\frac{p_i}{\rho_i}\left[1 - \left(\frac{p}{p_i}\right)^{(k-1)/k}\right] + W_i^2 + \omega^2(r^2 - r_i^2)} \tag{11}$$

Then the inviscid inverse design problem is solved and iterated with the boundary-layer calculation.

Based on the method described, a controlled diffusion cascade is designed and tested.[24] The main geometric parameters of the cascade designed are the chord length b = 90 mm, the pitch t = 58.37 mm, its maximum thickness C_{max} = 6.38 mm. The geometry of cascade and the comparison between the computed and the experimental distributions of the pressure coefficient for the inlet Mach number of 0.82 and p_2/p_1 = 1.177 are given in Figs. 13 and 14, respectively. The agreement seems quite good. It demonstrates that this method is effective for the design of a controlled diffusion cascade. The tested distributions of isentropic Mach number on the cascade surfaces at several different conditions are shown in Fig. 15. It is seen that in the supercritical cascade at the design condition, the shock appears for the conditions of M = 0.928 and of the positive incidence of 4 deg, and it remains shock-free at the negative incidence of −4 deg.

This example of the controlled diffusion cascade is also used to check and improve the solution method of the viscous inverse design problem using Navier–Stokes equation.[11] The experimental distribution of pressure coefficient is adopted as the

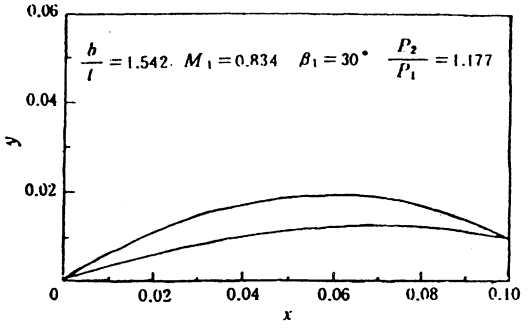

Fig. 13 Controlled diffusion cascade computed from the inverse problem.

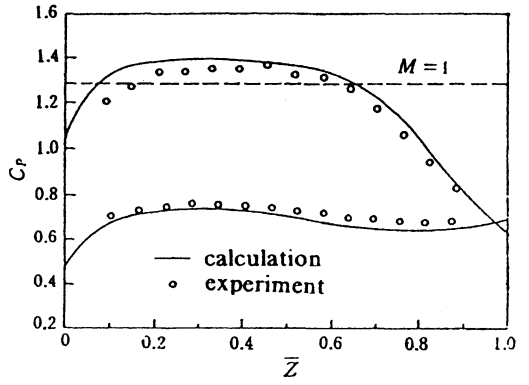

Fig. 14 Comparison of calculated and tested pressure coefficient distributions.

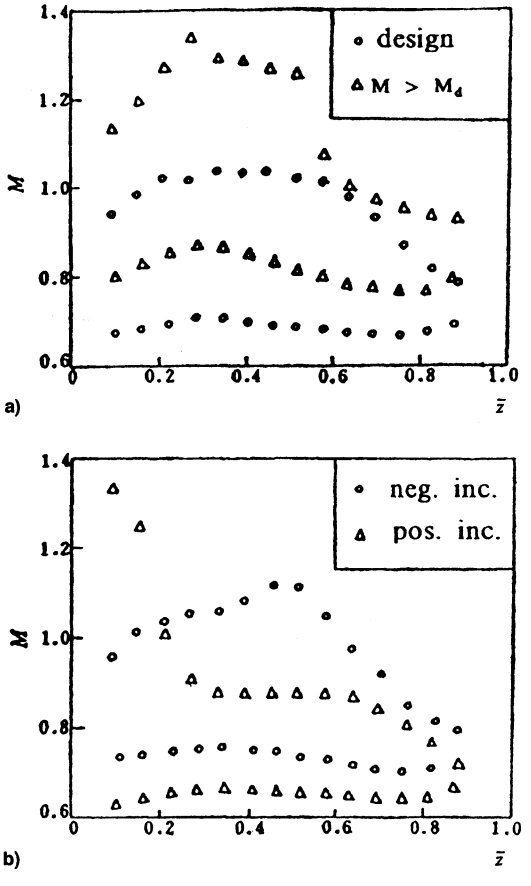

Fig. 15 Isentropic Mach number distributions at off-design conditions.

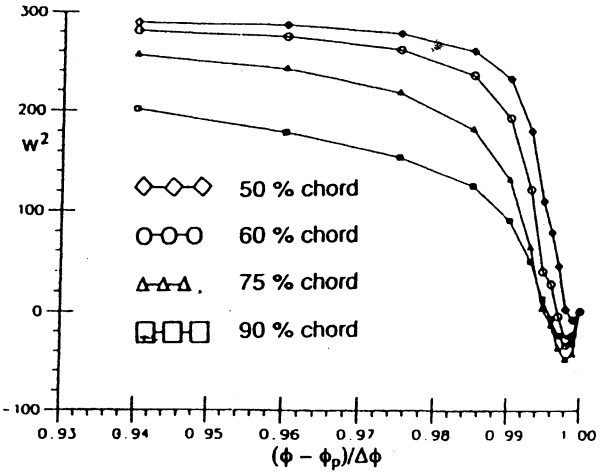

Fig. 16 Velocity profiles at different axial locations in the cascade channel.

target distribution, and the computed geometry of the cascade by this method coincides well with that of the test cascade (Fig. 16). It is interesting to note that the beginning of separation is located at 50% chord length. How to delay and reduce the shock strength is a problem to be solved in the future.

III. Application of the Theory of Design and Investigation of Turbomachinery

From the foregoing presentation and analysis of the three-dimensional flow theory in turbomachinery, it is seen that the theory provides the theoretical basis and the methods of solution for the aerothermodynamic design of turbomachinery. It perfectly combines the strictness in theory with the clear and definite physical meaning and with the reduced and simple calculation.

Based on the aerothermodynamic design system on three-dimensional flow theory, the design parameters are compared, adjusted, and improved during the process of convergence in the iterative solutions, and the whole aerothermodynamic arrangement becomes more reasonable. The course of iterative computation is the process of solving a three-dimensional flow, as well as the process of the aerodynamic design.

Usually the design from the calculation on the central S_2 surface according to the required pressure ratio, efficiency, and mass flow. Then, the computation along several surfaces of revolution are conducted to obtain the blade shape that may be determined by either solving a direct problem and choosing a standard cascade profile or solving an inverse design problem directly. The calculation may include the boundary-layer development. After stacking the coordinates of the blade, the stress analysis is needed and a full or a quasi-three-dimensional flow analysis is carried out, and the results obtained from this analysis are used to modify the design parameters and the aerodynamic arrangement. This procedure is repeated until a satisfactory design is obtained. In the complete aerothermodynamic design system based on the three-dimensional flow theory, the design criteria, which are extracted from synthesizing the basic theoretical analysis, the experimental results and the experience of the designer play an important role. They are continuously changed with the design method and the calculation method, and they are different from one company to another.

With the rapid development of computers and the continuous improvement of numerical methods in recent years, much progress has been made in solving three-dimensional Navier–Stokes equations directly. In the aerothermodynamic design system, the direct solutions of the three-dimensional Navier–Stokes equation have been included and is used to check the two-dimensional and quasi-three-dimensional nu-

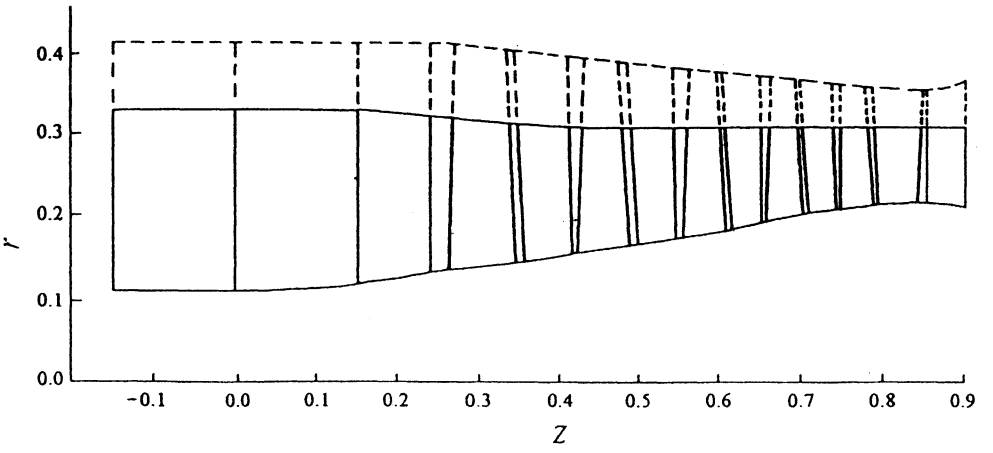

Fig. 17 Flow path of redesigning LP compressor of Spey aeroengine.

merical results. It is believed that it is playing an increasingly important role in the design.

As the example of the application of the three-dimensional flow theory to the design of turbomachinery, the CAS rotor, one part of a research single-stage transonic axial compressor, has been described and analyzed in detail,[1,2] and it is left out in the present paper. This theory and its numerical methods are also employed in the design or redesign of several civil and military fans, compressors, and turbines, and of a certain fluid turbomachinery. Several instances of this kind are given next.

Example 1. Tip-cut design of LP compressor for the Spey engine[25]: According to the requirements on the industrial Spey gas generator, the tip of blades of the LP compressor of a Spey aeroengine was cut out and the overall performance at n = 8000 rpm are the mass flow G = 54 kg/s, the pressure ratio π = 2.577, and the adiabatic efficiency η = 0.877. The problem is to determine the casing contour of the new compressor after cutting the tip of the original one.

The design is started from the calculations of the multistage central S_2 stream surface. Several different tip diameters are used to conduct the S_{2m} calculations. After comparing the numerical results with the design criteria defined in advance, a preliminary cutting size is decided and the results on its S_{2m} computation is supplied to the calculations on 11 surfaces of revolution. The variations of $V_\theta r$ and the thickness of S_2 stream filament along the streamlines on the S_1 surface are used for the next cycle of S_{2m} calculations. After five rounds of iterations of the calculations on a S_{2m} surface and the surfaces of revolution, the convergent solution of the quasi-three-dimensional flow is obtained and all design criteria are satisfied ultimately.

To ensure the off-design performance, some part-load working conditions are computed and the iterative calculations are completed in a similar way. The deviations of the inlet flow angle, the turning angle of the flow, and the Mach number from those of the original compressor are analyzed and the final tip flow path (Fig. 17) is determined. Figure 18 shows one of the calculated results. It gives a comparison of the inlet flow angle for the rotor 3 of the original and the tip-cutting Spey compressors. It is seen that the differences of the inlet flow angle for the two compressors are less than 5 deg, except the tip section at n = 3981 rpm. For the C4 cascade, such a difference is unable to significantly influence the performance of the compressor. The experiments confirm the conclusion of the calculation, G = 54.06 kg/s, π = 2.58, η = 0.889, and the surge margin is slightly increased.

Example 2. W-type centrifugal compressor[26]: The centrifugal compressor is a part of the combined compressor, which consists of several axial stages and one centrifugal stage. The centrifugal compressor was designed for a stagnation pressure ratio of 5.2 and a polytropic efficiency of 0.823. The inlet Mach number at the rotor tip was 1.15, the specific speed of rotation was 0.82, and the tangential speed at the rotor exit was 545 m/s. The surge margin of 15% is required, and the mass flow is 2.056 kg/s.

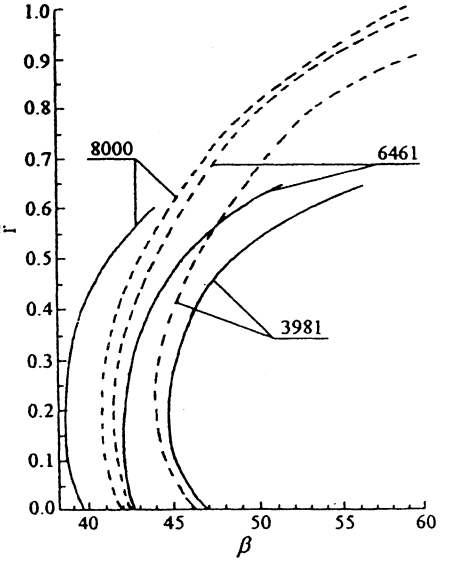

Fig. 18 Comparison of the inlet angles for the redesigning and original third rotors.

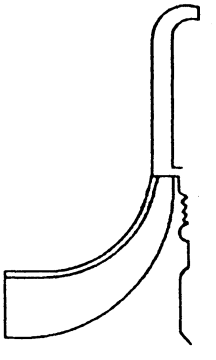

Fig. 19 Flow path of the centrifugal compressor.

As part of the combined compressor, the higher pressure ratio is advantageous to reduce the number of axial stages and to the matching with the latter.

The design also begins from the S_{2m} stream surface calculations. After more than 30 calculations, the flow path shown in Fig. 19 was tentatively selected, and the computation on several surfaces of revolution was followed. These procedures

were repeated until suitable results were obtained. At the same time the distributions of velocity were improved along the impeller surfaces. The blade coordinates on the surface of revolution were obtained according to the modified and improved distribution of velocity (Fig. 20) and the boundary-layer correction was considered.

To obtain an improved performance, the blades with lean forward and bend backward were used, and double row of radial diffuser with an inlet Mach number of 0.90 was adopted.

The test results of the test compressor show that at the design point the pressure ratio was 5.4, which was higher than the design target with 3.9%, and the efficiency and surge margin were 0.834 and 18.12%, respectively. They all exceeded the set index.

It is interesting to note that the computed static pressure at the impeller shroud agreed well with its experimental data. This fact indicates that there is no flow separation in the impeller.

All of these results deomonstrate that the aerothermodynamic design of this centrifugal compressor is successful and the calculations on two families of the stream surfaces are effective.

It is also noted that the tip clearance in the test compressor was 8.1%, which is excessively large. It is expected that if the tip clearance decreased to 4%, the efficiency may increase to 0.86 or so, and the surge margin would also be enlarged.

Example 3. The through-flow part of the redesigned 300/600 MW steam tubine[27]: The aerothermodynamic design system of the through-flow part consists of the quasi-three-dimensional flow calculations with the aid of two kinds of stream surfaces and the full three-dimensional flow check. The quasi-three-dimensional flow computation involves the solutions of both direct and inverse problems on the S_{2m} surface, and the solutions of the direct, inverse, and mixed-type problems with the boundary-layer correction on the surfaces of revolution. The full three-dimensional flow calculations are completed by means of the three-dimensional potential method and the methods of solving Euler equations and Navier–Stokes equations. For the S_{2m} calculation, the program can be used for the direct and inverse problem in both subsonic and transonic regions. In the S_1 direct problem, the finite volume LW scheme with the total variation diminishing property is adopted to the transonic flow computation, and in the S_1 inverse problem, the mean streamline method is utilized first and the stream function equation is solved by the relaxation method. In all of these computer codes the thermodynamic properties of the steam are used.[28] To accelerate the convergence of calculation the multigrid technique is added to these codes.

In the redesign some state-of-the-art technologies of steam turbine are applied. For the regulating stage of the high-pressure cylinder, the original straight blade with constant inner and outer radii is changed to the combined-lean blade with a convergent outer wall in the meridional plane. The coordinates of the new blade and the outer wall in the meridional plane are determined by means of the three-dimensional flow computation. The shape of the final combined-lean blade is given in Fig. 21. The outer surface of the blade is a cubic curve, and its stacking line consists of two straight lines and one circular arc. The experimental comparison of the loss coefficients for the original straight blade and the new blade (Fig. 22) shows that the loss of two end walls of the new one are decreased remarkably, and the average loss coefficient of the whole blade is 10.2%, which is much lower than the original one with a loss coefficient of 17.5%.

For the stages in the high- and medium-pressure cylinders and the front stages in the low-pressure cylinder, the three-dimensional controlled vortex design is used and the reactions along the blade height tend toward uniformity. In redesigning the last stage of the low-pressure cylinder the longer blade height (900 and 1000 mm) are selected and the quasi-three-dimensional flow calculation analysis and the full three-dimensional flow calculation check are combined in designing the blade. To reduce the loss caused by the shock-wave–boundary layer interaction, the front part of the suction surface of blade is investigated carefully and the resulting cascade and the distribution of Mach number are plotted in Fig. 23.[29]

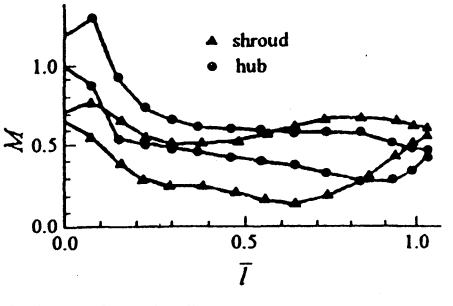

Fig. 20 Mach number distributions along the impeller surfaces.

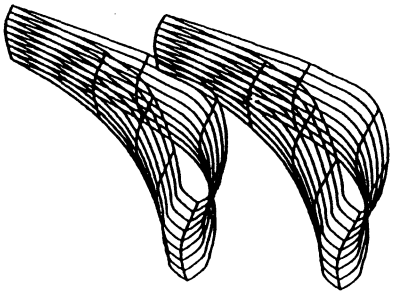

Fig. 21 Combined-lean blades.

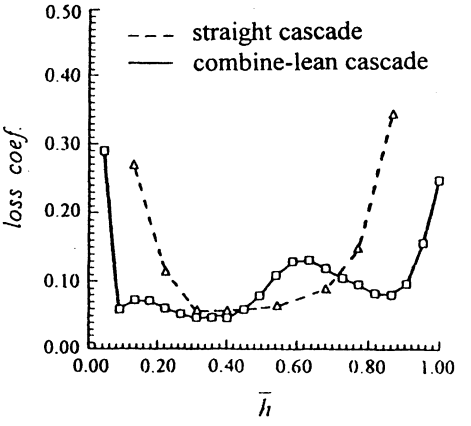

Fig. 22 Experimental loss coefficients.

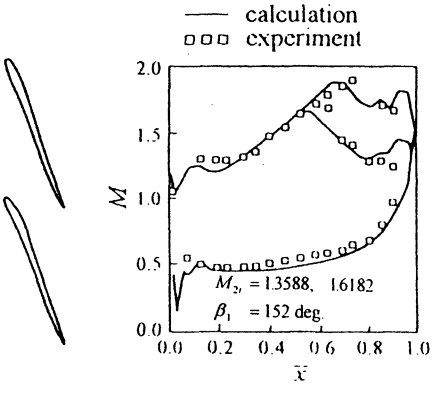

Fig. 23 Refined blade and Mach number distributions on its surfaces.

As expected, the thermal performance of the redesigned unit is significantly improved: the efficiency of the new steam turbine set is 5% higher than that of the original one.

IV. Conclusions

Over 40 years have passed since the first publication of the general theory of three-dimensional flow in turbomachinery. Now the theory has become a complete theoretical system and has given a significant impetus to the progress of the aeroengine and gas turbine. The quasi- and fully three-dimensional iterative solutions between S_1 and S_2 stream surfaces based on this theory has been developed and applied extensively. In China, several civil and military fans, compressors, and turbines, and some fluid turbomachinery were designed or redesigned successfully with this theory and its numerical methods.

It is believed that this theory will still play an important role in the design and investigation of the compressor, fan, turbine, and other turbomachinery.

References

[1]Wu, C. H., Zhao, X. L., and Qin, L. S., "Three-Dimensional Rotational Flow in Transonic Turbomachines: Part 2—Full Three-Dimensional Flow in CAS Rotor Obtained by Using a Number of S_1 and S_2 Streamfilaments," *Journal of Turbomachinery*, Vol. 114, No. 1, 1992.

[2]"Theory, Methods and Application of Three-Dimensional Flow Design of Transonic Axial Flow Compressor," *Chinese Journal of Engineering Thermophysics*, Vol. 1, No. 1, 1980.

[3]Zhao, X. L., "A Full 3D Iterative Solution in a Centrifugal Compressor Impeller," *Chinese Journal of Engineering Thermophysics*, Vol. 15, No. 3, 1994.

[4]Hua, Y. N., Yao, J., and Li, X. P., "Quasi Three-Dimensional Flow Analysis of a Centrifugal Compressor Impeller," CSET Paper 932016, 1993.

[5]Krain, H., "Swirling Impeller Flow," *Journal of Turbomachinery*, Vol. 110, No. 1, 1988.

[6]Krain, H., and Hoffmann, W., "Verification of an Impeller Design by Laser Measurements and 3D-Viscous Flow Calculation," American Society of Mechanical Engineers, Paper 89-GT-159, 1989.

[7]Cai, R., "Constraint on Design Parameters and Twist of Surface in Turbomachines," *Scientia Sinica (Series A)*, Vol. 26, No. 4, 1983.

[8]Wang, Z. M., "Inverse Design Calculation for Transonic Cascades," American Society of Mechanical Engineers, Paper 85-GT-5, 1985.

[9]Wang, Z. M., Chen, H. J., and Zhao, X. L., "A Quasi-3D Design Method of Transonic Compressor Blade with the Function of Improving Velocity Distribusion," *Proceedings of the 9th ISABE*, 1989, pp. 847–853.

[10]Wang, Z. M., "Solution of Cascade Inverse Problem Considering Viscous Influence," *Chinese Journal of Engineering Thermophysics (English Edition)*, Vol. 2, No. 2, 1990.

[11]Wang, Z. M., and Dulikravich, G. S., "A Numerical Method for Viscous Inverse Problem by Solving Navier-Stokes Equations," CSET Paper 942066, 1994.

[12]Ge, M. C., "A Stream Function Relaxation Method for Solving Blade Coordinates on S_1 Stream Surface," *Proceedings of the 7th ISABE*, 1985, pp. 482–486.

[13]Ge, M. C., Lou, Y. P., and Yu, Z. T., "A Method for Transonic Inverse Cascade Design with a Stream Function," *Journal of Turbomachinery*, Vol. 108, No. 2, 1986.

[14]Xu, J. Z., and Sun, X. Y., "A Method for Solving Inverse Aerodynamic Problem of Transonic Cascade," *Proceedings of the International Conference on Fluid Mechanics*, 1987, pp. 296–301.

[15]Ge, M. C., Yu, Z. T., and Lou, Y. P., "A New Approach to the Calculation of S_2 Stream Surfaces with Full Inverse and Hybrid Methods for Turbomachine," American Society of Mechanical Engineers, Paper 88-GT-262, 1988.

[16]Ge, M. C., and Lou, Y. P., "A Method for Solving Subsonic and Transonic Viscous Inverse Problem of Cascade with Stream Function Equations," *Chinese Journal of Engineering Thermophysics*, Vol. 8, No. 3, 1987.

[17]Zhu, G. X., and Ge, M. C., "Research on Inverse and Hybrid Problems for Axial, Mixed-Flow and Centrifugal Turbomachine on S_2 Surfaces with Given Meridional Velocities for Hub and Casing," *Chinese Journal of Engineering Thermophysics (English Edition)*, Vol. 2, No. 4, 1990.

[18]Liu, G. L., "Variational Principles and Generalized Variational Principles for the Hybrid Aerodynamic Problem of Airfoil Cascades on an Arbitary Streamsheet of Revolution," *Scientia Sinica (Series A)*, Vol. 23, No. 10, 1980.

[19]Liu, G. L., "A New Approach to Solve Hybrid Aerodynamic Problems of Airfoil Cascades on a General Streamsheet of Revolution," *Chinese Journal of Engineering Thermophysics*, Vol. 5, No. 1, 1983.

[20]Savage, M., Felix, A. R., and Emery, J. C., "High Speed Cascade Tests of a Blade Section Designed for Typical Hub Conditions of High-Flow Transonic Rotors," NACA RM L55F07, 1955.

[21]Chen, H. J., "On the Conservative From of Aerodynamic Equations of Turbomachinery," *Proceedings of the Conference in Memory of Professor Wu Chung-Hua*, 1993, pp. 113–121.

[22]Baldwin, B. S., and Lomax, H., "Thin Layer Approximation and Algebraic Model for Separated Turbulent Flows," AIAA Paper 78-257, 1978.

[23]MacCormack, R. W., "The Effect of Viscosity in Hypervelocity Impact Cratering," AIAA Paper 69-354, 1969.

[24]Wang, Z. M., Chung, Y. X., Wu, G. F., and Zhang, W., "Design and Testing of Shock-Free Supercritical Cascade," *Chinese Journal of Engineering Thermophysics*, Vol. 13, No. 4, 1992.

[25]Xu, J. Z., et al., "Aerothermodynamic Design and Calculation of Tip-Cutting LP Compressor of Spey Aeroengine," CSET Paper 83-40, 1983.

[26]Weng, D. Z., "Investigation of an Transonic Centrifugal Compressor," *Proceedings of the Conference in Memory of Professor Wu Chung-Hua* 1993, pp. 69–76.

[27]Jiang, H. D., Cai, R., et al., "Some Aerodynamic Features of Chinese Re-Designed 300/600 MW Steam Turbines, Part 1: Software System and Through-Flow Design," *Chinese Journal of Engineering Thermophysics*, Vol. 15, No. 2, 1994.

[28]Jiang, H. D., and Zhu, R. G., "S_2 Stream Surface Design Program for Steam Turbine," *Chinese Journal of Mechanical Engineering*, Vol. 26, No. 1, 1990.

[29]Mao, S. K., et al., "Some Aerodynamic Features of Chinese Re-Designed 300/600 MW Steam Turbines, Part 2: Blade Airfoil Optimization and Refinement," *Chinese Journal of Engineering Thermophysics*, Vol. 15, No. 3, 1994.